Medium-range atomic correlation in simple liquids. I. Distinction from short-range order

Chae Woo Ryu and Takeshi Egami

Phys. Rev. E **104**, 064109 — Published 9 December 2021

DOI: 10.1103/PhysRevE.104.064109

Medium-Range Atomic Correlation in Simple Liquid I: Distinction from Short-Range Order

Chae Woo Ryu[1] and Takeshi Egami[1,2,3]

[1]Department of Materials Science and Engineering, University of Tennessee, Knoxville, Tennessee 37996, USA

[2] Department of Physics and Astronomy, University of Tennessee, Knoxville, Tennessee 37996, USA

[3]Materials Sciences and Technology Division, Oak Ridge National Laboratory, Oak Ridge, Tennessee 37831, USA

Corresponding author: Takeshi Egami (egami@utk.edu)

ORCID identifier: T. Egami (0000-0002-1126-0276), C. W. Ryu (0000-0003-1588-4868)

Abstract

Physical properties of liquids and glasses are controlled not only by the short-range order (SRO) in the nearest neighbor atoms but also by the medium-range order (MRO) observed for atoms beyond the nearest neighbors. In this article the nature of the MRO as the descriptor of point-to-set atomic correlation is discussed focusing on simple liquids, such as metallic liquids. Through the results of x-ray diffraction and simulation with classical potentials we show that the third peak of the pair-distribution function, which describes the MRO, shows a distinct change in temperature dependence at the glass transition, whereas the first peak, which represents the SRO, changes smoothly through the glass transition. The result suggests that the glass transition is induced by the freezing of the MRO rather than that of the SRO, implying a major role of the MRO on the viscosity of supercooled liquid.

I. Introduction

The atomic structure of a crystalline solid is uniquely specified by the crystal symmetry, lattice constants, and several atomic position parameters within the unit cell, which can be determined through the Bragg diffraction by x-rays, neutrons and electrons. In contrast, liquids and glasses have no periodicity in the atomic structure, and accurate and meaningful description of their structures is a challenging task. Diffraction experiments provide only the information on two-body correlations, such as the pair-distribution function (PDF) [1 – 3], whereas often many-body correlations control their properties [4, 5]. This gap in knowledge has been a focus of intense research [6 – 9]. The goal of this work is to examine the possibility that certain features of the many-body correlations may be detected in the PDF, even though it depicts only the two-body correlations, and these features are related to critical properties, such as the glass transition. Our focus is limited to simple metallic liquids for which the PDF can be determined by experiment to distance much beyond the nearest neighbors.

The PDF, $g(r)$, is defined as,

$$g(r) = \frac{1}{4\pi N \rho_0 r^2} \sum_{i,j} \left\langle \delta\left(r - \left|\mathbf{r}_i - \mathbf{r}_j\right|\right) \right\rangle, \qquad (1)$$

where $\mathbf{r}_i$ is the atomic position of the i-th atom, N is the number of atoms in the system, ρ_0 is the average number density of atoms, and <….> denotes thermal and ensemble average. The PDF depicts the distribution of distances between two atoms. It can be determined by diffraction measurement through the Fourier-transformation of the structure function, $S(Q)$, where Q is the momentum transfer of scattering [1 – 3]. The PDF shows many peaks indicating multiple shell-like structures around each atom. The first peak describes the short-range order (SRO) in the nearest neighbor shell, whereas the peaks beyond the first peak depict the medium-range order (MRO).

Ornstein and Zernike were the first to propose a scheme to connect the SRO to the MRO through a self-consistency equation [10]. Slightly different approaches were suggested later by others [2, 3, 11, 12], but all these approaches are based on the idea that the MRO is directly tied to the SRO. However, there are important differences in nature between the SRO and the MRO [13 - 15]. The fundamental difference is that the SRO depicts the atom-atom correlations, whereas the MRO characterizes the correlations between an atom and a group of atoms. In other words, the

SRO represents the *point-to-point* correlations, whereas the MRO characterizes the *point-to-set* correlations [9]. Even though they are related, they are sufficiently distinct so that the behavior of the MRO cannot be readily predicted from the SRO alone, particularly in supercooled liquid. In this article we describe this difference based upon the results by x-ray diffraction and by molecular dynamics (MD) simulation on simple liquids with spherical interatomic potentials, and discuss the implications. We show that the temperature dependence of the MRO is distinct from that of the SRO, and the glass transition is defined by the freezing of the MRO, not that of the SRO.

II. Short- and medium-range order in liquid and glass

A. Point-to-point vs. point-to-set correlations

The first peak of the PDF describes the distribution of the nearest neighbor distances from the central atom. In liquids and glasses the number of neighboring atoms for each atom, the local coordination number, fluctuates from site to site. The average coordination number, $\bar{N}_C$, is given by the integration over the first peak of the PDF,

$$\bar{N}_C = 4\pi\rho_0 \int_{1st\ peak} g(r) r^2 dr \,. \tag{2}$$

For simple liquids with dense-random-packed (DRP) structure, such as metallic liquids, the value of $\bar{N}_C$ is 12 – 14 [16, 17]. At longer distances the PDF oscillates around unity, and its amplitude, $|g(r)-1|$, decays exponentially with distance as,

$$|g(r)-1| \approx \frac{\exp(-r/\xi_s)}{r}, \tag{3}$$

where ξ_s is the structural coherence length which characterizes the MRO. This form was suggested by Ornstein and Zernike through their self-consistency equation [10]. However, it is possible to arrive at this form from a more general point of view.

Because the SRO describes the atom-atom correlations, it reflects the atomic sizes of the constituent elements and the nature of chemical bonding among them. On the other hand, the width of the higher-order peaks in $g(r)$ which describe the MRO is significantly wider, of the order

of 1 Å, than that of the first peak. Each peak represents hundreds of atomic distances of which PDF peaks are overlapping to form a broad peak. Thus, the MRO peaks do not represent individual atomic distances, but instead they describe the point-to-set correlations between an atom and more coarse-grained local density fluctuations [7]. Therefore, even though the PDF represents just the two-body correlations it is possible that some features of the MRO reflect many-body correlations. For instance, the derivative of the PDF depends on the correlation among three-bodies, two atoms separated by r and the third atom at $r + dr$.

For crystalline materials it has been shown that the reduced PDF, $G(r) = 4\pi r \rho_0 \left[g(r) - 1 \right]$, has persistent oscillations with similar amplitudes up to macroscopic distances [18]. The argument for this behavior is as follows. At short distances the peak height and the width of the PDF are determined by the phonon amplitudes which increase with temperature. However, at large distances the PDF peaks overlap heavily even for crystals, so that each peak in $g(r)$ does not represent a single crystallographic distance any longer. Instead, it represents the number of atoms in the shell from r to $r + dr$, measured from the central atom, which is $N(r)dr$, where dr is the intrinsic peak width due to phonons. At large r, $N(r) = 4\pi\rho_0 r^2$, so the fluctuation, $dN(r)$, is equal to $2\sqrt{\pi\rho_0}r$. That is why $G(r)$ fluctuates with a fixed norm.

This argument applies equally well to liquids and glasses. Starting from an imaginary state with long-range density correlation, $G(r)$ should decay because of randomness in the structure of liquid as,

$$G(r) = G_0(r) \exp\left(-\frac{r}{\xi_s(T)} \right), \tag{4}$$

reproducing eq. (3), even without the Ornstein-Zernike theory. Here $G_0(r)$ describes the state with the limit of $\xi_s \to \infty$, the structurally coherent ideal glass state with long-range density correlation, and it has persistent oscillations in $G(r)$. Interestingly we were able to create a model with such a feature for $Pd_{42.5}Ni_{7.5}Cu_{30}P_{20}$ alloy liquid [19] with the Reverse Monte-Carlo (RMC) method [20], using the experimentally determined $G(r)$ as a starting point.

B. Variations of SRO and MRO with temperature

The difference in the nature between the SRO and the MRO is clearly seen in their variations with temperature. As shown in Fig. 1 the $G(r)$ of $Pd_{42.5}Ni_{7.5}Cu_{30}P_{20}$ liquid and glass determined by x-ray diffraction varies with temperature, with decreasing amplitudes of oscillations as temperature increases. The experimental details of this measurement are given in Ref. 19. The temperature dependences of the PDF peak heights are not uniform, and the first peak and the third peak show distinct behaviors. Fig. 2 shows the variation in the PDF peak height, $g(r_n, T) - 1$, with temperature, where r_n is the peak position of the n-th PDF peak, for the first three peaks (n = 1 – 3), for the experimental data for $Pd_{42.5}Ni_{7.5}Cu_{30}P_{20}$ and the simulation data for various alloy liquids studied in Ref. 19. The data are normalized by $g(r_n, T_g) - 1$, where T_g is the glass transition temperature, and plotted against T/T_g. For clarity the data are shifted down vertically by 0.2 for n = 2 and 0.4 for n = 3. The statistical error, $\Delta g/[g(r_n, T_g) - 1]$, for the experimental data for $Pd_{42.5}Ni_{7.5}Cu_{30}P_{20}$ is ±0.01 for the first peak and ±0.015 for the third peak. Other systematic errors affect the data evenly, and will have no or little effect on the normalized data. It is clear that the third peak shows a pronounced change in slope at T_g. In contrast, the first peak shows continuous variation without a noticeable change in slope at T_g for most liquid/glass. The data for the first peak of $Pd_{42.5}Ni_{7.5}Cu_{30}P_{20}$ show small change below T_g (~ 0.85 T_g), but not at T_g. The data for $Zr_{80}Pt_{20}$ are the only exception for the rule, for which the first peak shows a break in the slope, whereas the second peak smoothly changes through T_g. The continuous change in the height of the first peak through T_g was observed also by the previous x-ray diffraction study of $Zr_{50}Cu_{40}Al_{10}$ [21]. The second peak shows weaker, but notable changes at T_g, except for $Zr_{80}Pt_{20}$. To summarize, the ratio, $[g(r_3, T) - 1]/[g(r_1, T) - 1]$, is shown in Fig. 3 for all liquids we examined. It is clear that there is a distinct change in slope in the data at or near T_g, suggesting that the relationship between the SRO and the MRO is different above and below T_g.

The PDF peak height reflects phonon vibrations as well as the configurational changes. Because the density of states for phonons hardly changes through T_g [22], the increased slope in the temperature dependence of the height of the third peak above T_g must indicate that the MRO is largely frozen below T_g, but changes with temperature above T_g as expected for the structure of liquid [2, 3]. On the other hand, the continuous behavior of the first peak height suggests that the configurational change through the glass transition has virtually no effect on the SRO.

The PDF beyond the first peak which describes the MRO is approximately given by,

$$h(r) = g(r) - 1 \approx A_{MRO} \frac{a}{r} \sin\left(Q_{MRO} r + \delta_{MRO}\right) \exp\left(-\frac{r}{\xi_s}\right), \quad r > r_{cutoff} \ . \tag{5}$$

where a is the nearest neighbor distance defined by the first maximum in the PDF, δ_{MRO} is the phase factor, and r_{cutoff} is the position of the first minimum of the PDF beyond the first peak. Because the first peak of $S(Q)$ primarily depends on the MRO [14, 17], Q_{MRO} is very close to the position of the first peak of $S(Q)$, Q_1. Various arguments have been advanced proposing the SRO cluster as a building block and creating the MRO by stacking them [23 – 25]. In such a case the relevant length-scale is the cluster-cluster distance, which is a few times longer than the atomic distance. However, the periodicity of the MRO oscillations is slightly less than the interatomic distance. Therefore, the MRO discussed here cannot be explained in terms of the building of the SRO clusters.

The structural coherence length, ξ_s, varies with temperature, and obeys the Curie-Weiss law [15, 19]. The $\xi_s(T)$ shows a clear sign of change in slope around T_g [15, 19], and this is reflected to the behavior of the third peak of the PDF. This indicates that the MRO characterized by ξ_s freezes at T_g. In contrast, the height of the first peak of the PDF, $g(r_1)$, which describes the SRO, varies smoothly through T_g without freezing. The MRO amplitude, A_{MRO}, and the phase shift, δ_{MRO}, vary only weakly with temperature as shown in Figs. 4 and 5 for the experimental result on liquid $Pd_{42.5}Ni_{7.5}Cu_{30}P_{20}$ and for the simulation results for various liquid alloys studied in Ref. 19. These values are determined by fitting the eq. (5) to $G(r)$. The A_{MRO} and δ_{MRO} show small or no change in slope at T_g. Thus, the variation in the height of the third peak of the PDF largely reflects the change in $\xi_s(T)$ with temperature, with a pronounced slope change at T_g.

C. Dynamics of SRO and MRO

The disparate natures of the SRO and MRO manifest themselves also in the dynamic two-body correlation of atoms. The PDF is defined by the positions of two atoms at the same time; it is a thermal and ensemble average of the snapshots. However, the atomic correlations evolve with time, as described by the Van Hove function (VHF), $G(r, t)$, which is defined by the position of an atom at $t = 0$, $\boldsymbol{r}_i(0)$, and that of another atom at t, $\boldsymbol{r}_j(t)$ [26],

$$G(r,t)=\frac{1}{4\pi r^2\rho_0 N}\sum_{i,j}\left\langle \delta\left(r-\left|\boldsymbol{r}_i(0)-\boldsymbol{r}_j(t)\right|\right)\right\rangle. \tag{6}$$

The VHF can be obtained through the double-Fourier-transformation of the dynamic structure factor, $S(Q, \omega)$, measured by inelastic x-ray or neutron scattering [27, 28]. If the MRO is merely the extension of the SRO its dynamics must be just the convolution of the PDF with the self-part of the VHF which describes the motion of the central atom, and the VHF should decay with time uniformly with a single decay function [29]. However, de Gennes suggested that it might not be the case [30]. His prediction was then proven by the inelastic neutron scattering measurement by Brockhouse [27], and it is now known as de Gennes narrowing.

Whereas de Gennes narrowing is often regarded as the consequence of near neighbor dynamic interaction [31], recently we found a different explanation of this effect which ties it closely to the nature of the MRO as density fluctuations [32]. The argument to relate de Gennes narrowing to the near neighbor correlation [31] is based on the widely used assumption that the behavior of the first peak of $S(Q)$ at $Q = Q_1$ correspond to the behavior of the PDF at the distance $R_1 = 2\pi/Q_1$. However, this assumption is flawed because upon the Fourier-transformation the first peak of $S(Q)$ produces the higher-order peaks of $g(r)$ beyond the first peak, or the MRO, and not tied to the SRO [14, 17]. For instance, a delta-function in $S(Q)$ at Q_1,

$$S_0(\boldsymbol{Q})=\delta\left(|\boldsymbol{Q}|-Q_1\right), \tag{7}$$

produces a slowly decaying PDF,

$$g_0(r)-1=\frac{Q_1}{2\pi^2\rho_0}\frac{\sin(Q_1 r)}{r}. \tag{8}$$

When an exponential decay is added we obtain the form of eq. (3), and the first peak of $S(Q)$ becomes a Lorentzian [19]. Therefore, de Gennes narrowing reflects the dynamics of the MRO rather than that of the SRO.

Through molecular dynamics (MD) simulation it was found that the decay time of the VHF is linearly dependent on r in liquid at high temperatures [32]. The dependence varies with spatial dimensions, D, as,

$$\tau(r) = \tau_r \left(\frac{r}{r_1} \right)^{\chi} + \tau_0 , \tag{9}$$

where $\chi = (D\text{-}1)/2$ and r_1 is the nearest neighbor distance. This observation can be explained by the same argument used for explaining eq. (3) as discussed above. Because the higher-order peaks in $G(r, t)$ represent the coarse-grained density fluctuations their decay time is proportional to the number fluctuations, $dN(r) \sim r^{\chi}$, where $\chi = (D-1)/2$, with $\chi = 1$ for three dimensions [32]. This linear dependence of $\tau(r)$ on r indicates that de Gennes narrowing is a general property of any liquid, and is not indicative of collective dynamics of the atomic cage around an atom. It is quite pronounced even for high-temperature liquid in which atomic dynamics are largely uncorrelated [32]. It also shows that the MRO is not a mere consequence of the SRO, but it is a quantity with properties considerably distinct from those of the SRO. De Gennes narrowing characterizes the dynamics of the MRO, which is different from that of the SRO. It represents the dynamics of collective groups of atoms, not the individual atomic dynamics. For this reason, the MRO in the PDF and VHF describes the features of groups of atoms, beyond the pure two-body correlations.

III. Discussion

The contrast between the temperature dependence of the height of the third peak of the PDF, which characterizes the MRO, and that of the first peak of the PDF, which characterizes the SRO, demonstrates the important difference in the natures of the two. The result shows that the MRO freezes and goes out of equilibrium at T_g, whereas the SRO shows no sign of freezing. This implies that the MRO, not the SRO, reflects the change in viscosity. Indeed, the study on $Pd_{42.5}Ni_{7.5}Cu_{30}P_{20}$ liquid just above T_g [19] shows that the activation energy for viscosity, $E_a(T)$, defined by

$$\eta(T) = \eta_{\infty} \exp\left(\frac{E_a(T)}{k_B T} \right), \tag{10}$$

is related to ξ_S through,

$$E_a(T) = E_0 \left(\frac{\xi_s(T)}{a} \right)^3 . \tag{11}$$

Although this relationship needs to be confirmed for various liquids, it appears that the MRO is directly related to the viscosity of liquid. Furthermore, liquid fragility [33], defined by

$$m = \left. \frac{d \log \eta(T)}{d\left(T_g / T\right)} \right|_{T=T_g}, \tag{12}$$

where $\eta(T)$ is viscosity, is directly related to the structural coherence length at T_g by

$$\frac{m}{m_n} = n_c\left(T_g\right) = \rho_0 \left(\xi_s\left(T_g\right)\right)^3, \tag{13}$$

where m_n = 10.7 ± 1.1 for metallic liquids, m_n = 7.4 ± 0.4 for organic liquids, and 7.3 ± 1.2 for network liquids [34]. Because n_c is the number of atoms in the coherence volume, $V_c = \left(\xi_s(T)\right)^3$, this implies that the extent of cooperativity in the local deformation event determines fragility.

The observation that the MRO controls viscosity and fragility is in line with the argument by Bouchaud and Biroli [6] that the activation energy for viscosity is proportional to the volume defined by the cooperative regions. Montanari and Semerjian [7] generalized the argument from a broader perspective of dynamics in heterogeneous matter, and arrived at the same conclusion as an extreme case. Simulation studies [9, 35] show the presence of the point-to-set correlation length which is directly related to viscosity. Whether these length-scales are the same as $\xi_s(T)$ or not remains to be proven, but these results point to the possibility that viscosity is controlled by correlations at a medium-range length-scale, rather than the structure in the immediate neighborhood of an atom. Because the glass transition is defined by viscosity, it is reasonable to observe the MRO to freeze at T_g. In contrast, in a deeply supercooled liquid in which $\xi_s(T)$ is longer than the atomic distance, *a*, and strong dynamic heterogeneity is observed [4, 36 – 38] the medium surrounding the SRO is already nearly frozen in the timescale of the SRO fluctuations. Therefore, it is reasonable that the glass transition has no effect on the local dynamics of the SRO.

Furthermore, it is possible to justify this view from an even larger perspective [39]. Some time ago through simulation Rosenfeld proposed an idea that the transport properties of liquid was controlled by configurational entropy [40], expanding the entropy theory of Adam and Gibbs [41]. He chose the particle density as the parameter because he used the hard-sphere model. However,

the MRO is also related to the configurational entropy through the PDF [42 – 44]. The idea that liquid viscosity is determined by the MRO thus follows these preceding ideas.

On the other hand, this idea is at odds with the traditional view that viscosity is determined by structural defects [41, 45 – 47]. In crystalline solids defects are defined in terms of the anomalies in the topology of periodic atomic connectivity. When they move their identity does not change because they are topologically protected. However, in liquid and glass defects are not topologically protected, and change their structures upon motion. In particular, defects lose the memory of their thermal history at the saddle point of the potential energy landscape (PEL) [48], because they configurationally melt for a short time (~ 1 ps) [49]. Therefore, defects may indeed initiate local atomic rearrangement by breaking the atomic cage, but when the system reaches the saddle point it does not matter where atomic rearrangements started. The trajectory beyond the saddle point in the PEL is independent of thermal history [48], and unrelated to the defects which initiated atomic rearrangement. In other words, local atomic rearrangement may start from a defect, but it will be resisted by the MRO, and the final outcome is likely to be determined by the resistance by the MRO, rather than by the initiation of local atomic rearrangement. However, at the moment this scenario remains to be a plausible conjecture, and needs further examination.

Because ξ_S is linearly related to $S(Q_1)$ [14], $S(Q_1) - 1$ also follows the Curie-Weiss law [19]. The Curie-Weiss behavior of $S(Q_1)$ was predicted by the Ornstein-Zernike (OZ) theory at a high-temperature limit [50]. However, in this case the Curie temperature is positive for a system with an attractive potential, whereas our results show it is negative for all metallic liquids studied [19]. The apparent failure of the OZ theory is partly because the high-temperature approximation does not work for supercooled liquid. Also, the validity of the mean-field approximation in the OZ theory is questionable for supercooled liquid in which atoms are dynamically strongly correlated. Indeed, the difference between the temperature dependence for the SRO and that of the MRO is inconsistent with the OZ theory. According to the OZ theory, the structure function, $h(\boldsymbol{Q}) = S(\boldsymbol{Q}) - 1$, is given by,

$$h(\boldsymbol{Q}) = \frac{c(\boldsymbol{Q})}{1 - \rho_0 c(\boldsymbol{Q})}. \tag{14}$$

where ρ_0 is particle density, and $c(\boldsymbol{Q})$ describes the SRO [3, 10]. Therefore, a continuous variation of $c(\boldsymbol{Q})$ with temperature cannot produce the sharp changes in the slope of $S(Q_1) - 1$ and $\xi_s(T)$ at T_g. Thus, the observed Curie-Weiss behavior with a negative Curie temperature and the difference in the temperature dependence between the MRO and the SRO cannot be explained by the OZ theory. Furthermore, according to the eq. (14) $h(\boldsymbol{Q})$ and $c(\boldsymbol{Q})$ should have a peak at the same $\boldsymbol{Q}$, and the phase shift, δ_s, should be small or zero. However, it is significant for many alloys as shown in Fig. 3, suggesting that the MRO may not be directly linked to the SRO.

For a long time, the data on the structure of simple liquid were mostly limited to those for equilibrium liquids above the melting temperature [51], and there was dearth of data for supercooled liquids. Also because of the lack of precision in the PDF data the nature of the MRO has not been carefully examined. For this reason, the existing theories on liquid structure are oblivious to the difference in the nature between the SRO and the MRO for supercooled liquid. The perspective presented here based upon the data for deeply supercooled liquid through the glass transition present challenges to the existing theories on liquid structure.

IV. Conclusion

The medium-range order (MRO) in liquid and glass, defined by the atomic correlations beyond the nearest neighbors, has been considered to be directly tied to the short-range order (SRO) in the nearest neighbor atoms. Consequently, many research efforts focused on relating the properties of liquid and glass directly to the interatomic potential and the SRO [2, 3]. However, mounting evidence suggests that the MRO is distinct in nature from the SRO, and the relationship between them is indirect. Whereas the SRO describes the point-to-point correlation between atoms, the MRO depicts the point-to-set correlation between an atom and a group of atoms. Therefore, even though the PDF is a two-body correlation function, its oscillations in the medium-range catches more collective behavior of groups of atoms. In this article we discuss the differences between the temperature dependence of the SRO and that of the MRO in the experimental and simulation results, focusing on simple liquids, such as metallic liquids. We show that the temperature dependence of the MRO is distinct from that of the SRO. The glass transition is defined by the freezing of the MRO, not that of the SRO, implying that viscosity of supercooled

liquid is controlled by the MRO, rather than the SRO. The results provide an important piece of the puzzle on the origin of the glass transition, at least for simple liquids, such as metallic liquids. The extension to more complex liquids, including covalent liquids, is left for future work.

Acknowledgment

This work was supported by the US Department of Energy, Office of Science, Basic Energy Sciences, Materials Sciences and Engineering Division. The authors acknowledge W. Kob for useful discussion.

References:

1. B. E. Warren, *X-ray Diffraction* (Addison-Wesley, Reading, 1969).
2. P. A. Egelstaff, *An Introduction to the Liquid State* (First Edition, Academic Press, 1967, Second Edition, Oxford University Press, 1991).
3. J.-P. Hansen, I. R. McDonald, *Theory of Simple Liquids* (Academic Press, 1976, 1986, 2006).
4. S. C. Glotzer, V. N. Novikov and T. B. Schröder, *J. Chem. Phys.* **112,** 509 (2000).
5. S. Albert, Th. Bauer, M. Michl, G. Biroli, J. P. Bouchaud, A. Loidl, P. Lunkenheimer, R. Tourbot, C. Wiertel-Gasquet and F. Ladieu, *Science* **352,** 1308 (2016).
6. J.-P. Bouchaud and G. Biroli, *J. Chem. Phys.* **121,** 7347 (2004).
7. A. Montanari and G. Semerjian, *J. Stat. Phys.* **125,** 23 (2006).
8. L. Berthier and G. Biroli G, *Rev. Mod. Phys.* **83,** 587 (2011).
9. L. Berthier and W. Kob, *Phys. Rev. E* **85,** 011102 (2012).
10. L. S. Ornstein and F. Zernike, *Proc. Roy. Netherlands Acad. Arts Sci. (KNAW)* **17**, 793 (1914).

11. J. S. Rowlinson, *Rep. Prog. Phys*. **28,** 169 (1965).

12. J. K. Percus and G. J. Yevick, *Phys. Rev.* **110,** 1 (1958).

13. T. Egami, *Front. Phys.* **8**, 50 (2020).

14. C. W. Ryu, W. Dmowski and T. Egami, *Phys. Rev. E* **101,** 030601(R) (2020).

15. T. Egami and C. W. Ryu, *Front. Chem.* **8,** 579169 (2020).

16. J. D. Bernal and J. Mason, *Nature* **188,** 910 (1960).

17. G. S. Cargill, III. *Solid State Phys.* **30**, 227 (1975).

18. V. A. Levashov, S. J. L. Billinge and M. F. Thorpe, *Phys. Rev. B* **72,** 024111 (2005).

19. C. W. Ryu, W. Dmowski, K. F. Kelton, G. W. Lee, E. S. Park, J. R. Morris and T. Egami, *Sci. Rep.* **9**, 18579 (2019).

20. R. L. McGreevy, *J. Phys.: Condens. Matt.* **13,** R877- R913 (2001).

21. K. Georgarakis, L. Hennet, G. A. Evangelakis, J. Antonowicz, G. B. Bokas, V. Honkimaki, A. Bytchkov, M. W. Chen and A. R. Yavari, *Acta Mater.* **87**, 174 (2015).

22. H. L. Smith, C. W. Li, A. Ho, G. R. Garrett, D. S. Kim, F. C. Yang, M. S. Lucas, T. Swan-Wood, J. Y. Y. Lin, M. B. Stone, D. L. Abernathy, M. D. Demetriou and B. Fultz, *Nature Phys.* **13,** 900 (2017).

23. D. B. Miracle, *Nature Mater.* **3,** 697 (2004).

24. H. W. Sheng, W. K. Luo, F. M. Alamgir, J. M. Bai and E. Ma, *Nature*, **439,** 419 (2006).

25. C. P. Royall and S. R. Williams, *Phys. Rep.* **560,** 1 (2015).

26. L. Van Hove, *Phys. Rev*. **95**, 249 (1954).

27. B. N. Brockhouse and N. K. Pope, *Phys. Rev. Lett.* **3**, 259 (1959).

28. T. Iwashita, B. Wu, W.-R. Chen, S. Tsutsui, A. Q. R. Baron and T. Egami, *Sci. Adv.* **3**, e1603079 (2017).

29. G. H. Vineyard, *Phys. Rev.* **110,** 999 (1958).

30. P. G. de Gennes, *Physica*, **25**, 825 (1959).

31. P. Kleban, *J. Stat. Phys.* **11,** 317 (1974).

32. B. Wu, T. Iwashita and T. Egami, *Phys. Rev. Lett.* **120**, 135502 (2018).

33. C. A. Angell, *Science* **267**, 1924 (1995).

34. C. W. Ryu and T. Egami, *Phys. Rev. E* **102,** 042615 (2020).

35. W. Kob, S. Roldán-Vargas and L. Berthier, *Nature Phys.* **8,** 164 (2012).

36. W. Kob, C. Donati, S. J. Plimpton, P. H. Poole and S. C. Glotzer, *Phys. Rev. Lett.* **79,** 2827 (1997).

37. C. Donati, J. F. Douglas, W. Kob, S. J. Plimpton, P. H. Poole and S. C. Glotzer, *Phys. Rev. Lett.* **80,** 2338 (1998).

38. A. Widmer-Cooper and P. Harrowell, *Phys. Rev. Lett.* **96,** 185701 (2006).

39. J. C. Dyre, *J. Chem. Phys.* **149,** 210901 (2018).

40. Y. Rosenfeld, *Phys. Rev. A* **15,** 2545 (1977).

41. G. Adam and J. H. Gibbs, *J. Chem. Phys.* **43,** 139 (1965).

42. D. C. Wallace, *J. Chem. Phys.* **87,** 2282 (1987).

43. A. Baranyai and D. J. Evans, *Phys. Rev. A* **40,** 3817 (1989).

44. D. M. Nicholson, C. Y. Gao, M. T. McDonnell, C. C. Sluss and D. J. Keffer, *Entropy* **23,** 234 (2021).

45. M. H. Cohen and D. Turnbull, *J. Chem. Phys.* **31,** 1164 (1959).

46. E. D. Cubuk, S. S. Schoenholz, J. M. Rieser, B. D. Malone, J. Rottler, D. J. Durian, E. Kaxiras and A. J. Liu, *Phys. Rev. Lett.* **114,** 108001 (2015).

47. V. Bapst, T. Keck, A. Grabska-Barwińska, C. Donner, E. D. Cubuk, S. S. Schoenholz, A. Obika, A. W. R. Nelson, T. Back, D. Hassabis and P. Kohli, *Nature Physics* **16,** 448 (2020).

48. Y. Fan, T. Iwashita and T. Egami, *Nature Commun.*, **8,** 15417 (2017).

49. J. Ding, L. Li, N. Wang, L. Tian, M. Asta, R. O. Ritchie and T. Egami, *Materials Today Physics*, **17,** 100359 (2021).

50. S. Chakrabarty and Z. Nussinov, *Phys. Rev. B* **84,** 064124 (2011).

51. E. Donth, *The glass transition: Relaxation dynamics of liquids and disordered materials* (Springer, Berlin, 2010).

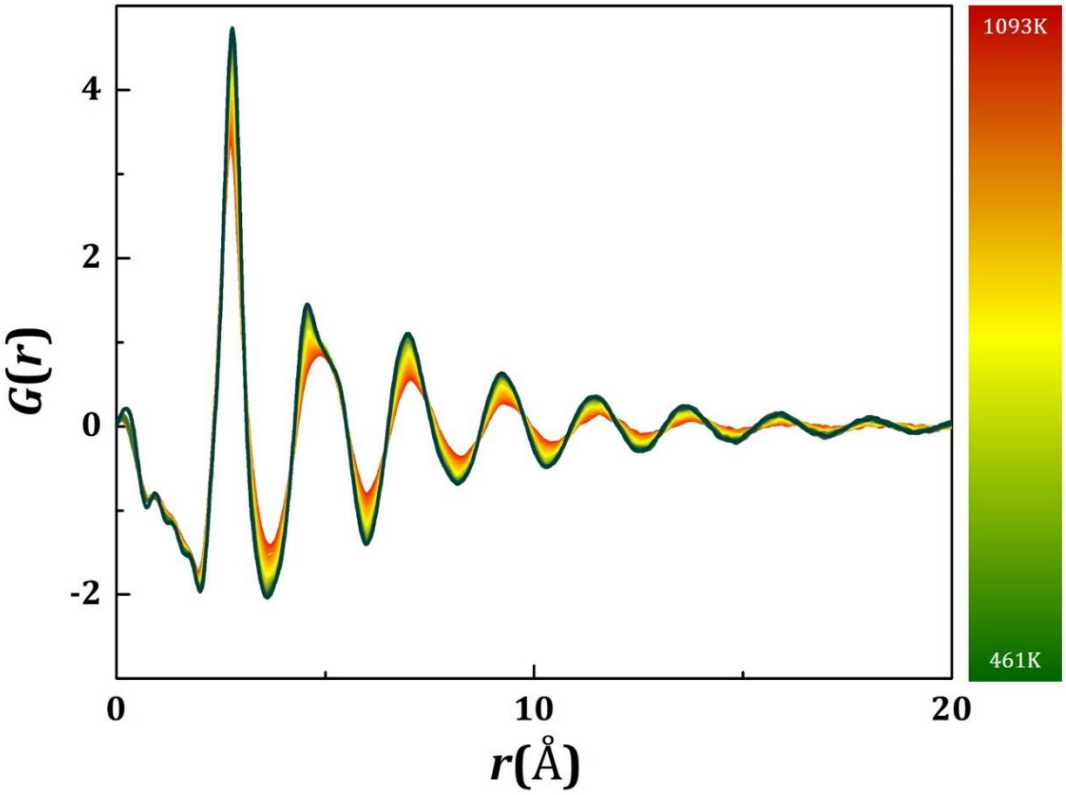

Fig. 1 The reduced PDF, $G(r)$, for $Pd_{42.5}Ni_{7.5}Cu_{30}P_{20}$ liquid and glass at various temperatures from 461K to 1093K, determined by x-ray diffraction with electrostatic levitation. The glass transition temperature is 573K.

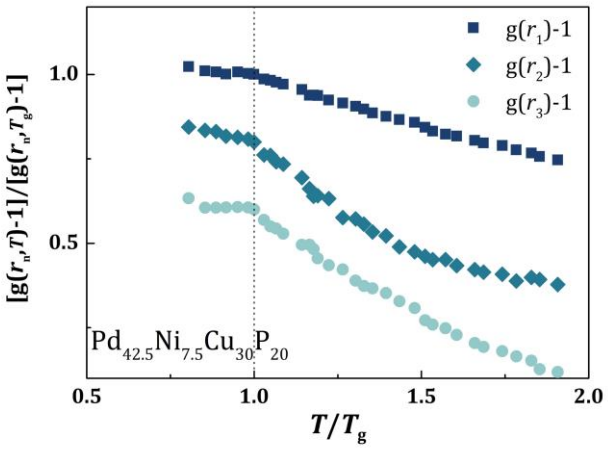
g(r_1)-1
g(r_2)-1
g(r_3)-1
[g(r_n,T)-1]/[g(r_n,T_g)-1]
T/T_g
$Pd_{42.5}Ni_{7.5}Cu_{30}P_{20}$

(a)

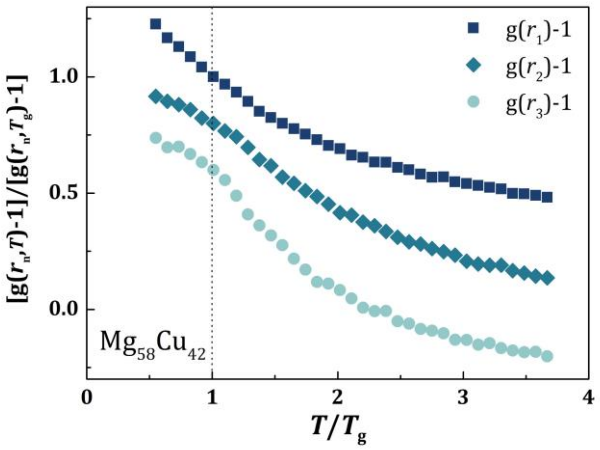
g(r_1)-1
g(r_2)-1
g(r_3)-1
[g(r_n,T)-1]/[g(r_n,T_g)-1]
T/T_g
$Mg_{58}Cu_{42}$

(b)

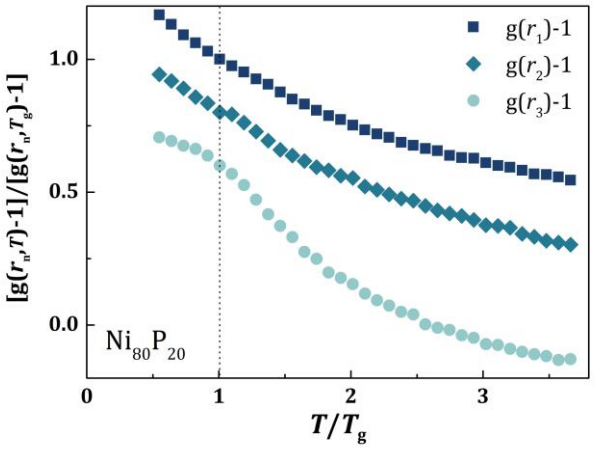
g(r_1)-1
g(r_2)-1
g(r_3)-1
[g(r_n,T)-1]/[g(r_n,T_g)-1]
T/T_g
$Ni_{80}P_{20}$

(c)

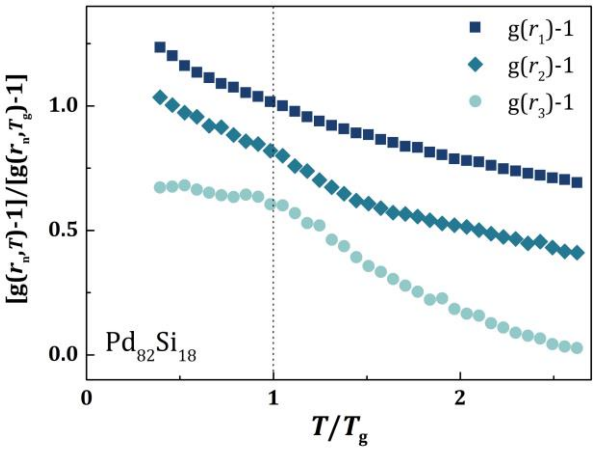
g(r_1)-1
g(r_2)-1
g(r_3)-1
$[g(r_n,T)-1]/[g(r_n,T_g)-1]$
1.0
0.5
0.0
0
1
2
T/T_g
$Pd_{82}Si_{18}$

(d)

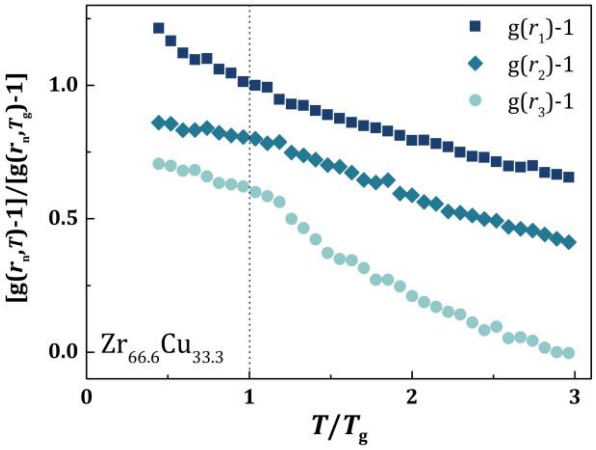
g(r_1)-1
g(r_2)-1
g(r_3)-1
$[g(r_n,T)-1]/[g(r_n,T_g)-1]$
1.0
0.5
0.0
0
1
2
3
T/T_g
$Zr_{66.6}Cu_{33.3}$

(e)

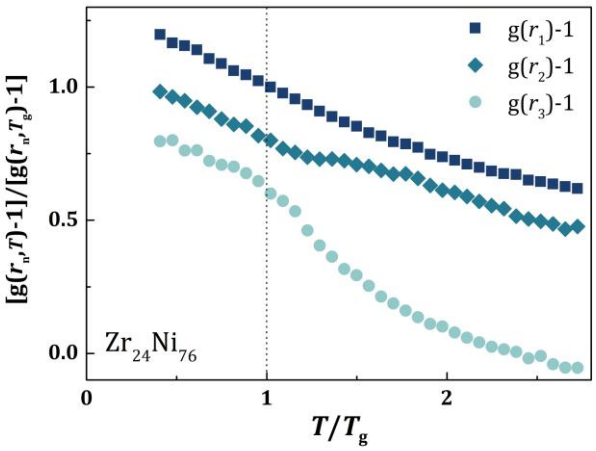
g(r_1)-1
g(r_2)-1
g(r_3)-1
$[g(r_n,T)-1]/[g(r_n,T_g)-1]$
1.0
0.5
0.0
0
1
2
T/T_g
$Zr_{24}Ni_{76}$

(f)

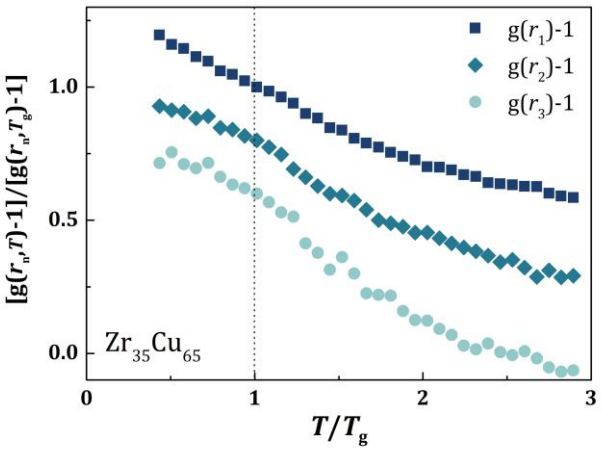
g(r_1)-1
g(r_2)-1
g(r_3)-1
$[g(r_n,T)-1]/[g(r_n,T_g)-1]$
$Zr_{35}Cu_{65}$
T/T_g

(g)

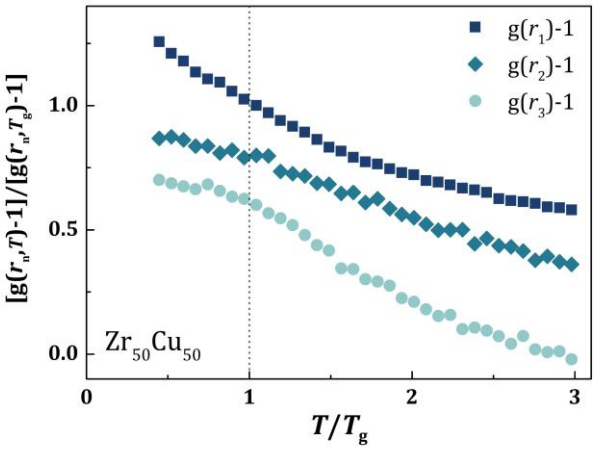
g(r_1)-1
g(r_2)-1
g(r_3)-1
$[g(r_n,T)-1]/[g(r_n,T_g)-1]$
$Zr_{50}Cu_{50}$
T/T_g

(h)

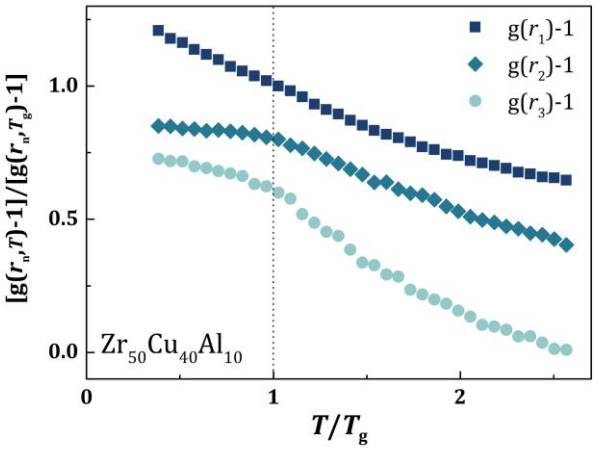
g(r_1)-1
g(r_2)-1
g(r_3)-1
$[g(r_n,T)-1]/[g(r_n,T_g)-1]$
$Zr_{50}Cu_{40}Al_{10}$
T/T_g

(i)

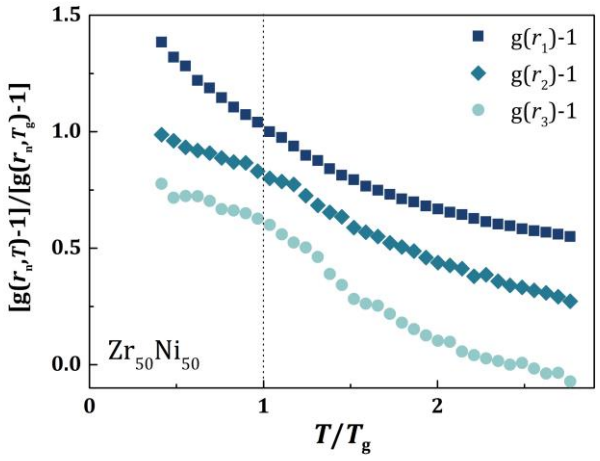
1.5
1.0
0.5
0.0
0
1
2
T/T_g
$[g(r_n,T)-1]/[g(r_n,T_g)-1]$
$g(r_1)$-1
$g(r_2)$-1
$g(r_3)$-1
$Zr_{50}Ni_{50}$

(j)

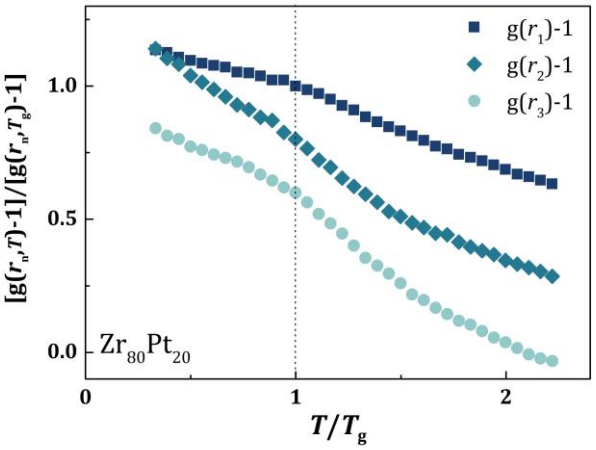
1.0
0.5
0.0
0
1
2
T/T_g
$[g(r_n,T)-1]/[g(r_n,T_g)-1]$
$g(r_1)$-1
$g(r_2)$-1
$g(r_3)$-1
$Zr_{80}Pt_{20}$

(k)

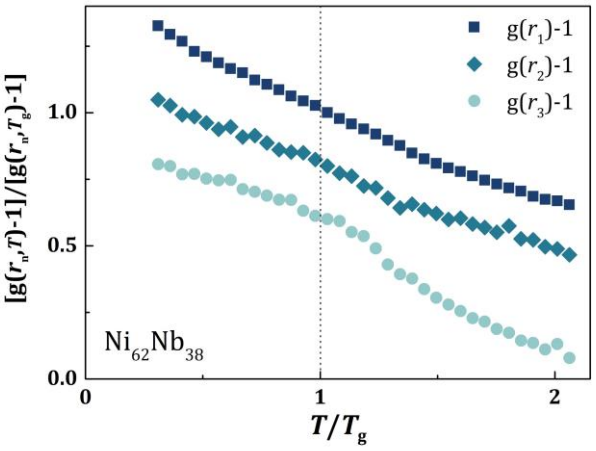
1.0
0.5
0.0
0
1
2
T/T_g
$[g(r_n,T)-1]/[g(r_n,T_g)-1]$
$g(r_1)$-1
$g(r_2)$-1
$g(r_3)$-1
$Ni_{62}Nb_{38}$

(l)

Fig. 2. The height of the first three peaks of the PDF as a function of T/T_g for (a) experimental result on liquid $Pd_{42.5}Ni_{7.5}Cu_{30}P_{20}$ and (b) for simulation results on various liquid alloys. The data are vertically shifted by 0.2 for n = 2 and 0.4 for n = 3 to avoid overlaps.

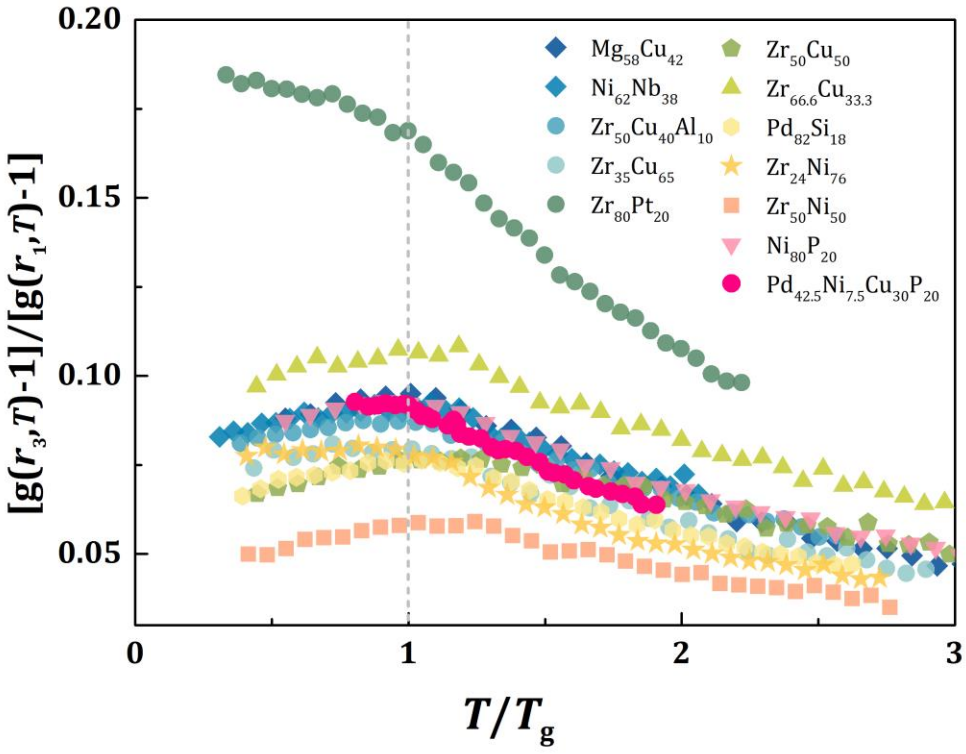

Fig. 3. The ratio, $[g(r_3,T)-1]/[g(r_1,T)-1]$, for all liquids shown in Fig. 2.

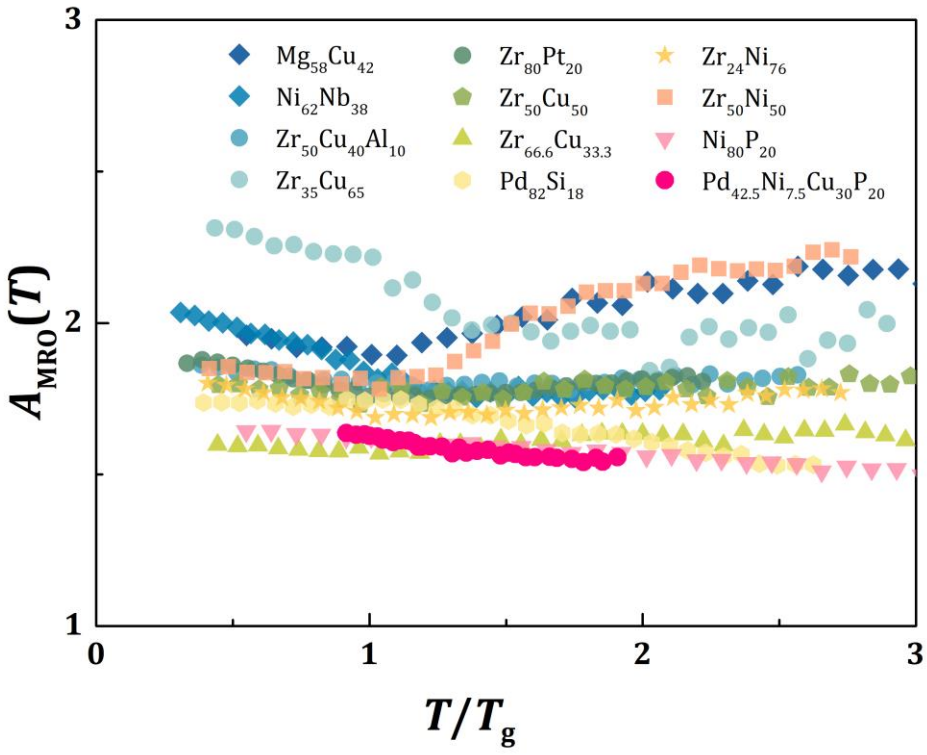

Fig. 4. Temperature dependence of the MRO amplitude, $A_{MRO}(T)$, as a function of T/T_g for the experimental result on liquid $Pd_{42.5}Ni_{7.5}Cu_{30}P_{20}$ and for the simulation results for various liquid alloys.

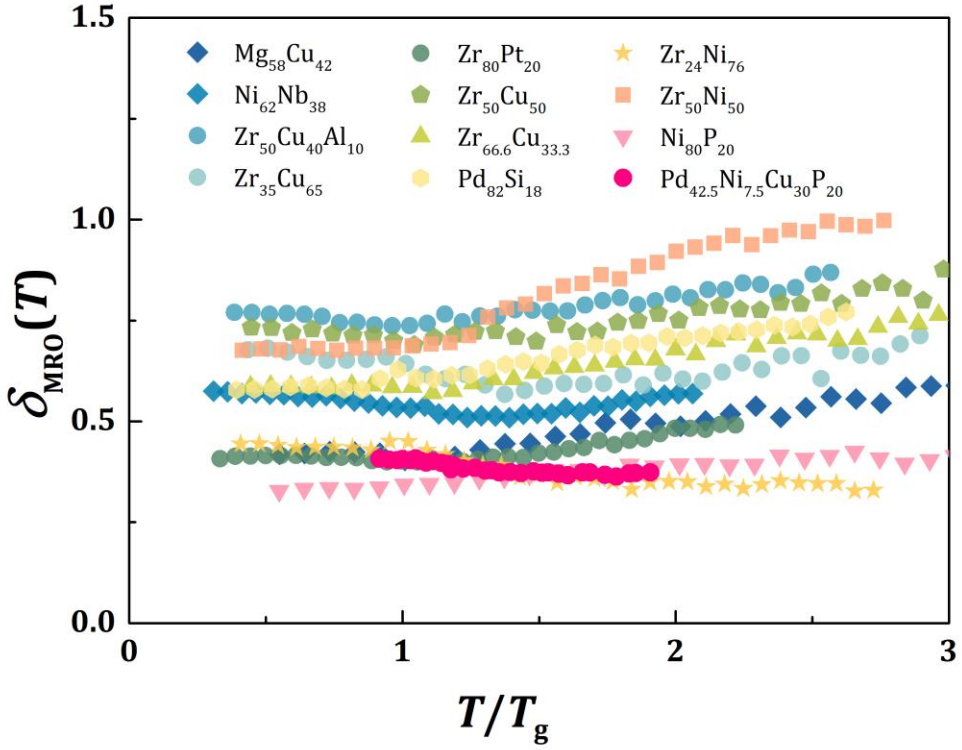

Fig. 5. Temperature dependence of the MRO phase shift, $\delta_{MRO}(T)$, as a function of T/T_g for the experimental result on liquid $Pd_{42.5}Ni_{7.5}Cu_{30}P_{20}$ and for the simulation results for various liquid alloys.